Journal of the European Ceramic Society 17 (1997) 565–573

PII: S0955-2219(96)00092-1
0955-2219/97/$17.00

Pressureless Sintering and Elastic Constants of Al_2O_3–SiC 'Nanocomposites'

C. C. Anya & S. G. Roberts*

University of Oxford, Department of Materials, Parks Road, Oxford OX1 3PH, UK

(Received 6 March 1996; revised version received 15 April 1996; accepted 3 May 1996)

Abstract

A study is presented of how to obtain very near theoretical densities (≥99·6%) in Al_2O_3–SiC 'nanocomposites' by pressureless sintering. Several factors are considered in order to achieve the optimal densification. The most important factors are: good dispersion of SiC particles in the matrix, cold-isostatic pressing of green samples and use of a relatively coarse-sized bedding powder (which allows efficient effusion of carbon monoxide from the sample), correct choice of sintering temperature (which depends on the size of alumina particles), and the use of a nitrogen atmosphere during sintering.

The elastic constants of the nanocomposites produced depend on the degree of densification. About 2% reduction from theoretical density leads to about a 6% reduction of the Young's modulus. The experimentally obtained moduli are correlated with three models that relate porosity to Young's modulus.

1 Introduction

The significantly higher strength of Al_2O_3–SiC (nano-sized particles) composites, relative to monolithic Al_2O_3, is now well established.[1–3] Generally, such composites have been fabricated to high densities by hot-pressing routes. For many potential applications of these materials, hot-pressing would be prohibitively expensive, and pressureless sintering routes would be preferable if near full density could be achieved. Borsa *et al.*[3] fabricated Al_2O_3–5% SiC composites by a pressureless sintering route to a maximum of about 96% of the theoretical density, and Zhao *et al.*[2] sintered a 5% SiC composite to 98·3% theoretical density by the same route. However, Zhao *et al.*[2] noted that in pressureless sintering small differences in the processing procedure and variables can have a pronounced effect on the microstructure (and ultimately the properties) of sintered bodies.

This paper reports an exploration of the effects of some sintering variables on the final density and resultant Young's modulus of Al_2O_3–SiC composites with 5%, 10% and 15% (by volume) of 'nano'-size SiC particles. The variables studied were:

(1) the particle size of the alumina;
(2) the sintering temperature;
(3) the method of blending the composite powder; and
(4) the type of gas used during the sintering process.

This exploration has led to a 'recipe' for the production of near fully dense composites by pressureless sintering. In a recent paper,[4] we reported that the fracture toughness (K_{Ic}) of these pressureless sintered composites is, on average, about 65% better than that of monolithic alumina of the same grain size.

2 Materials and Experimental

Two types of α-Al_2O_3, AES 11c (Mandoval, UK) and AKP 53 (Sumitomo, Japan), were used; these are referred to below as AES and AKP. The particle size of AES is 400 nm, while that of AKP is 200 nm. The SiC powder used was UF-45 (Lonza, Germany). The characteristics of these powders, as given by the suppliers, are listed in Table 1.

Al_2O_3 and SiC powders were attrition-milled in deionized water with ZrO_2 balls for 2 h to obtain 0, 5, 10 and 15 vol% SiC in alumina. To promote the dispersion of SiC powder (which was preagitated ultrasonically for about 10 min) in the slurry, about 15 drops (2 ml) of Dispex A40 dispersant (Allied Colloids, UK) were added. The attrition-milled mixtures were then freeze-dried.

SiC usually has a surface film of silica-rich phase of variable thickness. Some authors[5] suggest that the oxidation of SiC through its reaction with

*To whom correspondence should be addressed.

Table 1. Characteristics of raw materials

	α-Al_2O_3(AES)	α-Al_2O_3 (AKP)	α-SiC (Lonza 45)	Added C
Al_2O_3 (wt%)	99·9	99·995	0·03	—
SiO_2 (wt%)	0·04	0·0016	—	—
Fe_2O_3 (wt%)	0·01	0·001	—	—
Na_2O (wt%)	0·03	0·0002	—	—
MgO (wt%)	0·04	0·0004	—	—
Cu (wt%)	—	>0·001	—	—
CaO (wt%)	0·02	—	—	—
Mean particle size (μm)	0·4	0·2	0·2	—
Density (g cm ^{3})	3·96	3·986	3·2	—
Free C (wt%)	—	—	0·58	—
Fe_2O_4 (wt%)	—	—	0·05	—
Si metal (wt%)	—	—	0·22	—
O_2 (wt%)	—	—	3·5	—
Ash (wt%)	—	—	—	3
Extractable phosphate (wt%)	—	—	—	0·5

this film [reaction (1) below] leads to non-optimal mechanical properties of the composites. To suppress this reaction, some powder mixes had 0·8 wt% added carbon (Aldrich, UK; see Table 1) so as to promote the thermodynamically favoured reaction (2):

$$2SiO_2 + SiC \rightarrow 3\ SiO + CO \quad (1)$$

$$SiO_2 + C \rightarrow SiO + CO \quad (2)$$

As well as preventing the SiC from reacting with SiO_2, we also wished to investigate what effect any contaminating carbon (from powder processing and furnace linings), or the CO generated by reaction (2), could have on the sintering process.

Dried powders were uniaxially consolidated with about 20 MPa (to facilitate handling), and then isostatically cold-pressed (CIP-ed) at 140 MPa.

A graphite-lined furnace (Astro Industries Inc., CA, USA) and SiC powder bedding were used. Two different particle sizes of the SiC bedding powder — 600 and 120 grit sizes — were used. The 120 grit size was used only for the composite with added carbon. After exploratory experiments to determine optimal sintering temperatures and times, 1700 and 1775°C for 4 h were used.

Smith *et al.*[5] observed that a static atmosphere promotes better mechanical properties than a flowing atmosphere. For this reason only static atmospheres were used here. Coble[6] argues that nitrogen is better than argon in the sintering of alumina. The effect of these two gases was investigated on 5 and 10 vol% SiC–Al_2O_3 (AES) blends.

For comparison, monolithic AES alumina powder was also sintered at 1560°C for 3 h in air, using the same alumina powder as the bed. The aim was to obtain the same degree of densification and grain size as in the composites. The monolithic alumina was also attrition-milled, freeze-dried and CIP-ed at 140 MPa before sintering. Attempts to sinter the alumina in a reducing atmosphere (as used for the composites) resulted in a low density product. (Another study of the sintering behaviour of alumina[7] also concluded that a reducing atmosphere is harmful).

Density measurements were carried out in deionized water by Archimedes' principle. Ground and polished composite samples were etched so as to observe grain structures, using orthophosphoric acid at about 250°C and by thermal etching (in both argon and vacuum) at 1400°C for 1·5 h. Thermal etching led to oxidation of the SiC particles, while chemical etching left the particles intact. The alumina sample was thermally etched in air at 1400°C for 2 h. The grain structure of the alumina sample was further studied using transmission electron microscopy (TEM; Philips CM 20). Grain sizes were determined by the linear intercept method. Elastic constants — Young's modulus (E), shear modulus (G) and Poisson's ratio (ν) — were determined using a Grindosonic instrument (MK4i).

3 Results and Discussion

Table 2 gives a summary of the various sintering schedules used and the grain sizes obtained. Table 3 shows the elastic constants of the samples. A comparison of the experimental values of E with those calculated according to different models using the observed volume fraction of pores (see Section 3·6) is given in Table 4. We discuss below the effects of the experimental variables on the densification of the composites.

3.1 Powder beds

The low density of sample 3 (with added carbon) in Table 2 is due to poor evacuation of the gases produced according to eqn (2). The SiC bed here was 600 grit size. The fineness of the powder bed

Table 2. Sintering schedules and results

Serial no.	*vol% SiC*[a]	*Al_2O_3 particle size (nm)*	*Sintering temp. (°C)*	*Dwell time (h)*	*Power bed*	*Atmosphere*	*Density (g cm^{-3})*	*Density (% th)*	*Grain size (μm)*[b]
1	0	400	1560	3	Al_2O_3	Air	3·96	99·9	3·5 ± 1·3
2	5	400	1775	4	SiC, 600 grit	N_2	3·91	99·8	4 ± 1·1
3	5, wc	400	1775	4	SiC, 600 grit	N_2	3·67	93·6	4·8 ± 0·7
4	5, wc	400	1775	4	SiC, 120 grit	N_2	3·85	98·2	nd
5	5	200	1775	4	SiC, 600 grit	N_2	3·92	99·2	6·3 ± 2·3
6	5	200	1700	4	SiC, 600 grit	N_2	3·95	99·9	3·2 ± 0·6
7	5	400	1775	4	SiC, 600 grit	Ar	3·85	98·2	nd
8	10	400	1775	4	SiC, 600 grit	N_2	3·87	99·7	2·9 ± 0·5
9	10	400	1775	4	SiC, 600 grit	Ar	3·81	98·2	nd
10	15	400	1775	4	SiC, 600 grit	N_2	3·83	99·6	2·6 ± 0·3
11	5	400	1700	4	SiC, 600 grit	N_2	3·87	98·7	nd
12	10	400	1700	4	SiC, 600 grit	N_2	3·69	95·1	nd
13	15	400	1700	4	SiC, 600 grit	N_2	3·52	91·5	nd

[a]Mixtures without carbon, except wc = with carbon.
[b]nd = Not determined.

led to poor effusion of gases from the sample, and the sample appeared bloated (Fig. 1). Sintering the same batch with a coarser SiC powder bed (120 grit), sample 4, improved the achieved density to 3·85 g cm^{-3}, 98·2% of the theoretical density of 5 vol% SiC composite. Figure 2 illustrates this effect clearly.

Figure 3 shows thermally etched samples of 5 vol% SiC–AES alumina composite, sintered under identical conditions, with carbon [sample 4, Fig. 3(a)] and without carbon [sample 2, Fig. 3(b)]. The small holes correspond to oxidized SiC particles. Figure 4 shows the same samples etched in orthophosphoric acid. Although the chemical etching gives exaggerated grain boundary widths and a rather poor appearance (due to the re-emergence of etchant trapped in surface pores or in crevices[8]), the SiC particles remain intact, and show as small points of bright contrast.

Figures 3 and 4 suggest that the samples with added carbon show more uniformity in grain size distribution. Samples with carbon have a slightly larger grain size of 4·4 ± 0·7 μm, compared with 4·0 ± 1·1 μm of those without carbon. The relatively non-uniform grain size distribution of the samples without added carbon can be explained on the basis of the thickness of the SiO_2-rich film on the SiC particles. As this varies, so also will be the extent to which the SiC particles are oxidized according to eqn (1) above. Grain facets with thick SiO_2 films will tend to oxidize the SiC particles that would impede grain boundary motion.

Table 3. Elastic properties of AES alumina and composites

Material	*Sintering gas*	*Density (% th)*	E *(GPa)*	G *(GPa)*	*ν*
Al_2O_3	Air	99·9	397·4 ± 3	160 ± 2	0·249
5 vol% SiC/Al_2O_3	N_2	99·8	399·5 ± 4	159 ± 1	0·254
5 vol% SiC/Al_2O_3	Ar	98·2	381·1 ± 3	152 ± 1	0·241
10 vol% SiC/Al_2O_3	N_2	99·7	407·2 ± 2	162·5 ± 2	0·25
10 vol% SiC/Al_2O_3	Ar	98·2	386·8 ± 2·5	154·7 ± 1·5	0·24
15 vol% SiC/Al_2O_3	N_2	99·6	409·5 ± 4	165 ± 1	0·237

Table 4. Comparison of experimental Young's moduli with modelled values

Material	*Sintering gas*	*Porosity p (vol %)*	E *(GPa)*	*Predicted* E *(GPa)*		
				Phani[15] *[eqn (3)]*	*Duckworth*[16] *[eqn (4)]*	*Wang*[17] *[eqn (5)]*
Al_2O_3	Air	0·1	397·4 ± 3	397·9	398·2	400·6
5 vol% SiC/Al_2O_3	N_2	0·2	399·5 ± 4	398·9	399·5	404·3
5 vol% SiC/Al_2O_3	Ar	1·8	381·1 ± 3	350·9	357·1	398·0
10 vol% SiC/Al_2O_3	N_2	0·3	407·2 ± 2	399·8	400·7	408·0
10 vol% SiC/Al_2O_3	Ar	1·8	386·8 ± 2·5	354·5	360·8	402·0
15 vol% SiC/Al_2O_3	N_2	0·4	409·5 ± 4	400·7	401·9	411·7

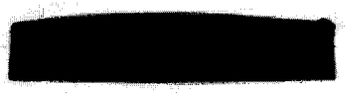

Fig. 1. Optical micrograph of bloated sample (25 mm diameter) of 5 vol% SiC composite (with added C) sintered using SiC powder bed of 600 grit size.

The addition of carbon did not improve the degree of densification, and its positive effect on grain size distribution may not be significant in improving mechanical properties. However, where there is the possibility of CO generation, for example by the presence of traces of carbon in the mixture in mixtures milled with organic liquids and/or sintering in graphite-lined furnaces, attention must be given to the particle size of the bedding powder. Even if it is assumed that calcining at lower temperatures burns out all the organics, it has been demonstrated[9] that sintering in graphite-lined furnaces generates CO, above about 1200°C, by the oxidation of some of the graphite linings. CO entrapment in pores after pore closure has been shown[10] to retard the densification of crystalline oxides. A related effect appears to act in our materials (compare specimens 2 and 5 in Table 2).

3.2 Attrition-milling/freeze-drying

Figure 4 shows that a uniform distribution of SiC particles was achieved within 2 h by attrition-milling in deionized water. The freeze-drying, which follows immediately after milling, ensures that the particles are frozen in at their respective positions without a tendency to flocculate. Good distributions of SiC particles were also obtained in 10 and 15 vol% SiC–AES alumina composites, which had average grain sizes of 2·9 ± 0·5 μm and 2·6 ± 0·3 μm respectively (Fig. 5).

The use of this attrition-milling/freeze-drying method makes the use of organic liquids (which could contaminate the mixture) unnecessary. Attrition-milling also drastically reduces the time used for blending the powders; a typical blending

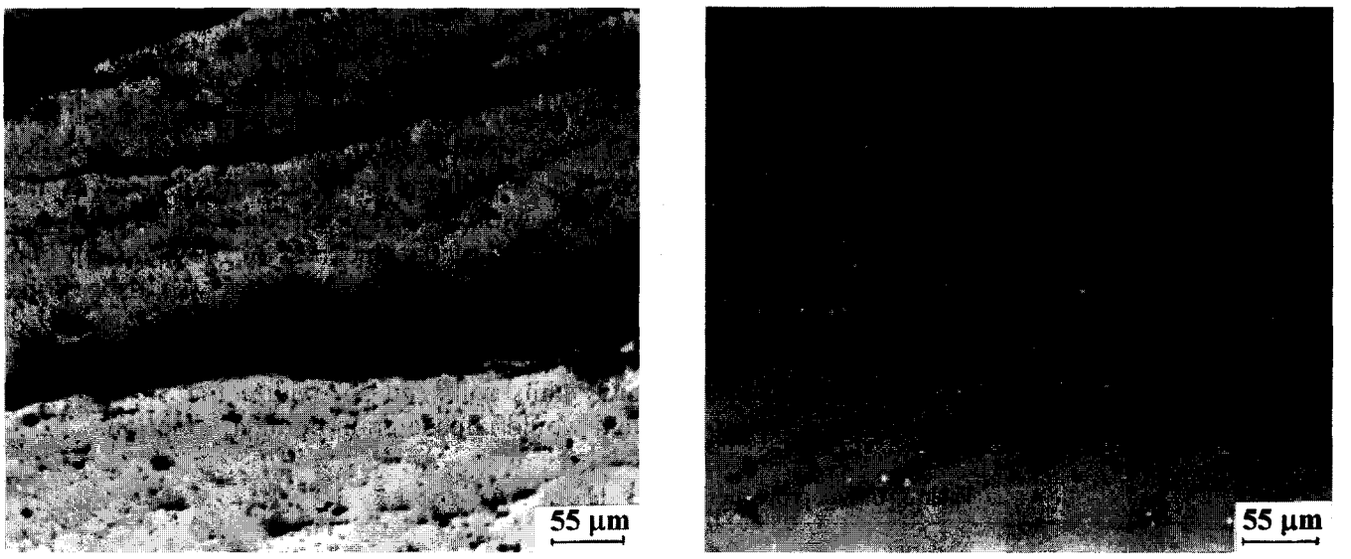

(a) (b)

Fig. 2. Optical images of polished samples of 5 vol% SiC composites (with added C) sintered using SiC bed of grit size 600 grit (a) and 120 grit (b).

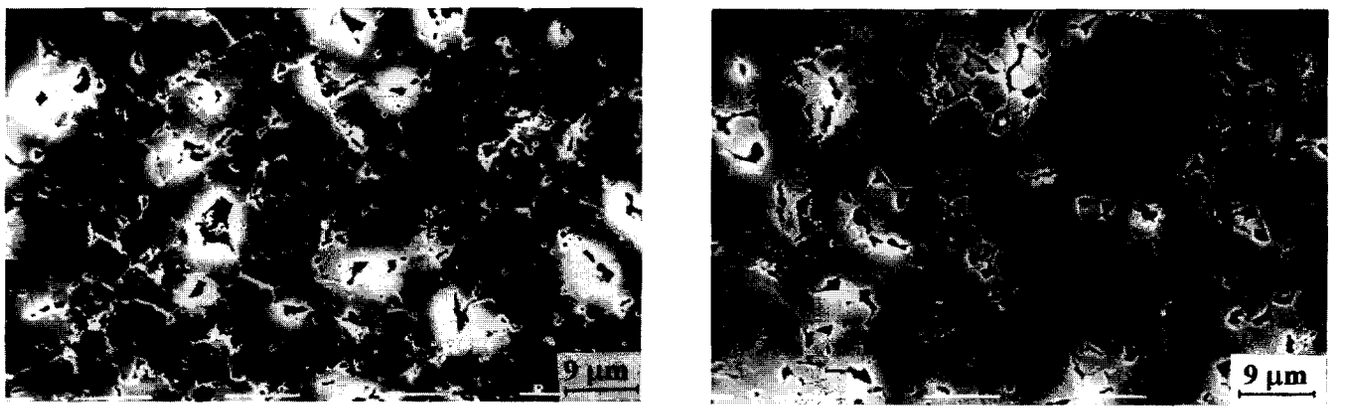

(a) (b)

Fig. 3. SEM micrographs of AES alumina/5 vol% SiC composite thermally etched at 1400°C for 1·5 h: (a) with added carbon prior to sintering; (b) without added carbon. Note the greater uniformity of grain size distribution of (a) relative to (b).

time in a ball mill is about 48 h.[2] This short process time also considerably reduces the possibility of contamination by the material of the balls used in attrition-milling.

3.3 Effect of sintering atmosphere

Figure 6 shows typical micrographs of polished 5 vol% SiC composite sintered under the same conditions in nitrogen [Fig. 6(a)] and in argon [Fig. 6(b)] atmospheres, samples 2 and 7 respectively in Table 2.

The nitrogen atmosphere gives better densification. Coble[6] argued that gases which (albeit very negligibly) are chemically active with the solid are more soluble than inert gases, and so have a higher diffusivity. 'Active' gases will thus provide less resistance to final pore closure. However, we did not find any data in the literature on the solubility of these two gases in alumina and/or SiC. Another similar explanation could be that nitrogen is more soluble (and/or diffuses more readily) in the silica-rich intergranular phases.

3.4 Sintering temperature, SiC fraction and Al_2O_3 particle size

Temperatures lower than 1775°C lead to lower densities. At 1700°C all the composites made with 400 nm alumina showed reductions in densification, of about 1% for 5 vol% SiC, 5% for 10 vol% SiC and 8% for 15 vol% SiC (samples 11, 12 and 13 in Table 2).

It is possible that the optimal sintering temperature might depend on the volume fraction of the SiC particles, since the degree of densification decreases slightly with increasing volume fraction of SiC particles at 1775°C (samples 6, 8 and 10 in Table 2). However, the variation in final density with SiC volume fraction is higher for samples sintered at 1700°C (samples 11, 12 and 13 in Table 2).

To achieve a given shrinkage, a powder with smaller particles should require a lower sintering temperature, due to the increased surface area and surface energy per unit volume.[11] The 5 vol% SiC composite with AKP alumina (200 nm particle size) was sintered at 1775 and 1700°C. A density of 99·2% was achieved at 1775°C, while at 1700°C this rose to 99·9% (samples 5 and 6 respectively in Table 2). The 1775°C sample has a grain size of 6·3 ± 2·3 μm [Fig. 7(a)], while that sintered at 1700°C has a grain size of 3·2 ± 0·6 μm [Fig. 7(b)].

The pressureless sintering temperature of these materials must thus be closely matched with the particle size. A small increase in sintering temperature

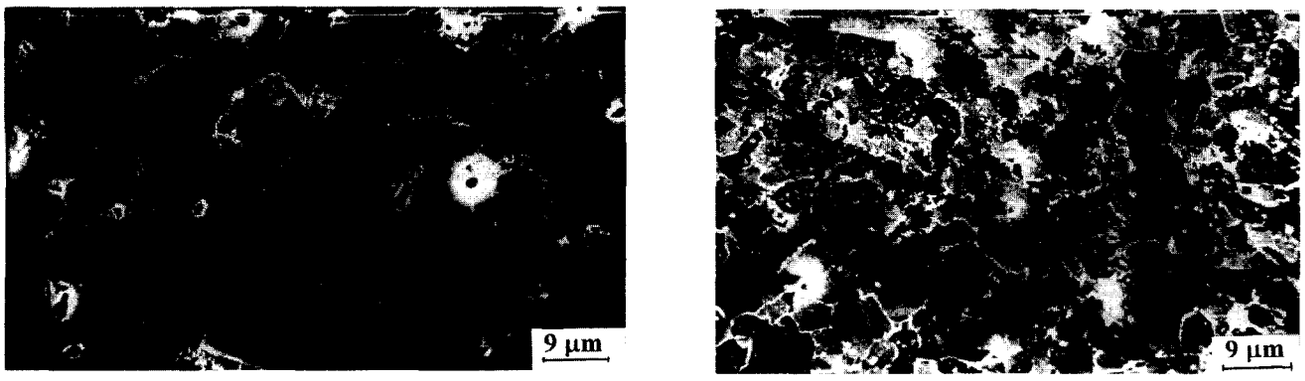

(a) (b)

Fig. 4. SEM micrographs of the same sample as in Fig. 3, but thermally etched with H_3PO_4 acid; (a) with carbon; (b) without carbon. Note the presence of SiC particles, unlike in Fig. 3.

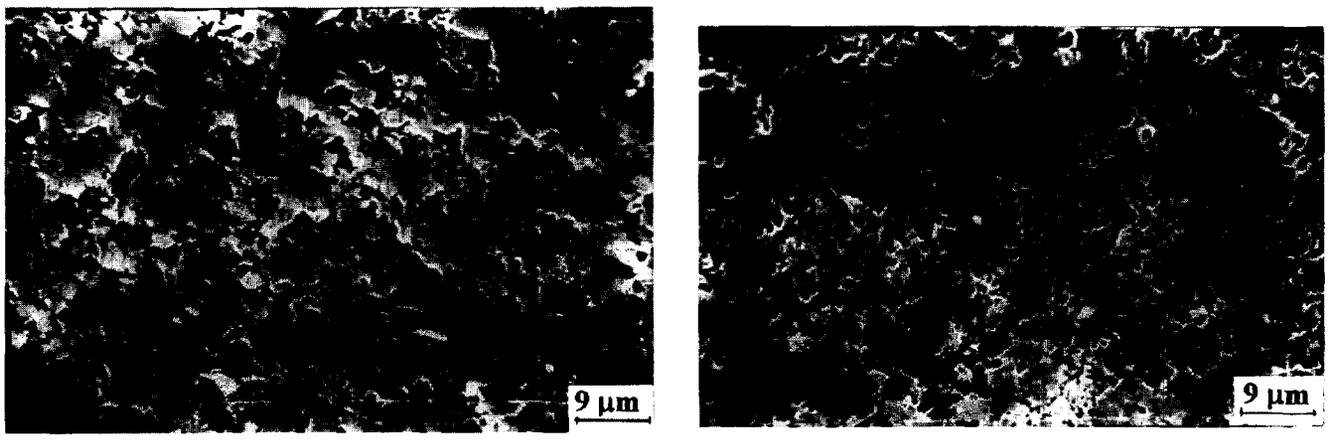

(a) (b)

Fig. 5. Distribution of SiC particles in alumina (AES) matrix for composites with 10 vol% SiC (a) and 15 vol% SiC (b).

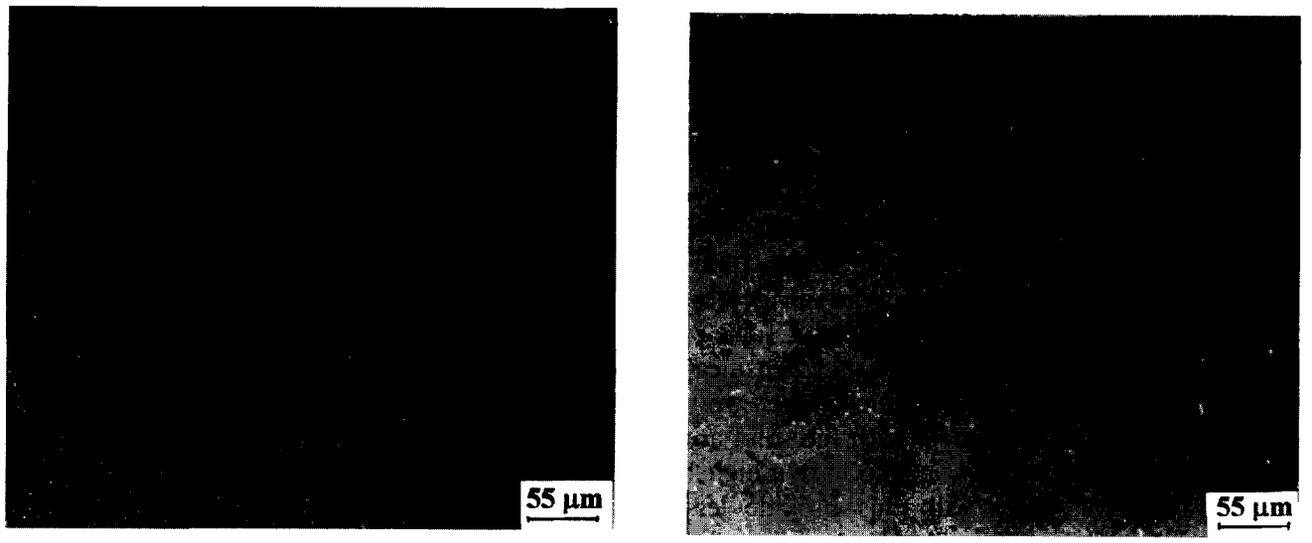

Fig. 6. Optical micrographs of polished 5 vol% SiC/AES alumina composite showing the degree of densification in samples sintered in atmospheres of (a) nitrogen (the Vickers indent is unrelated to this paper) and (b) argon. Note the level of porosity in the composite sintered in argon.

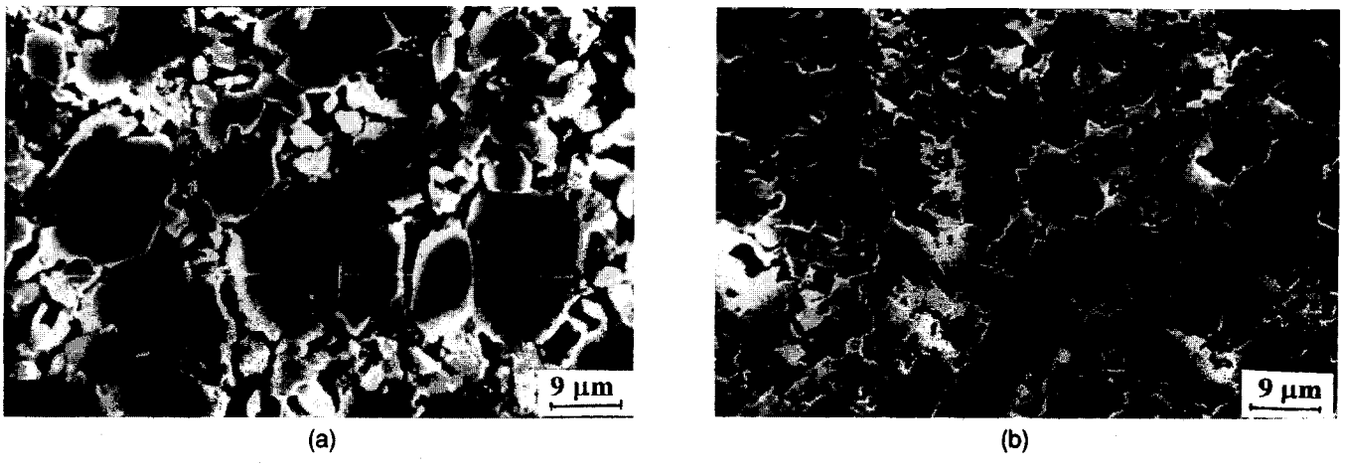

Fig. 7. SEM micrographs showing the relationship between sintering temperature and alumina particle size of 5 vol% SiC/alumina (AKP) composite: (a) sintered at 1775°C — compare with Fig. 4(b) (same volume fraction of SiC in a 400 nm size matrix powder and sintered at the same temperature for the same duration); (b) sintered at 1700°C.

for the 200 nm alumina gives a near doubling of the average grain size. The slightly lower density obtained for the 5 vol% SiC–200 nm AKP alumina composite sintered at 1775°C may be connected with abnormal grain growth.[12]

3.5 Abnormal grain growth

The grain size distribution for the sample made from the 200 nm AKP powder at 1775°C is relatively non-uniform, which suggests abnormal grain growth has occurred [Fig. 7(a)]. This did not occur for material made from the 400 nm AES powder, sintered at the same temperature [Fig. 4(b)]. The absence of abnormal grain growth in the 400 nm alumina may be due to its higher MgO content, about 100 times greater than in the 200 nm alumina (see Table 1). MgO is believed[13] to suppress abnormal grain growth by reducing the mobility difference between unwet grain boundaries (by solid-solution pinning) and those wet by an intergranular liquid film.

However, the 400 nm alumina showed abnormal grain growth, with varying grain aspect ratios, when sintered without SiC at 1560°C [Fig. 8(a)]. Therefore the higher MgO content of this powder is not solely responsible for suppressing abnormal grain growth in the 5 vol% SiC–400 nm alumina composite sintered at 1775°C. Of the several grains investigated in the TEM, two are shown in Fig. 8. Aspect ratios >3 were found [Fig. 8(c)]. In contrast, Borsa *et al.*[3] obtained an equiaxed grain structure by hot-pressing this AES alumina powder at 1400°C for 1 h. This suggests that, irrespective of a powder's composition, hot-pressing, with its relatively low temperatures and shorter dwell times, is capable of suppressing abnormal grain growth. For some applications, say for enhanced flaw tolerance,[14] where these high aspect ratios are

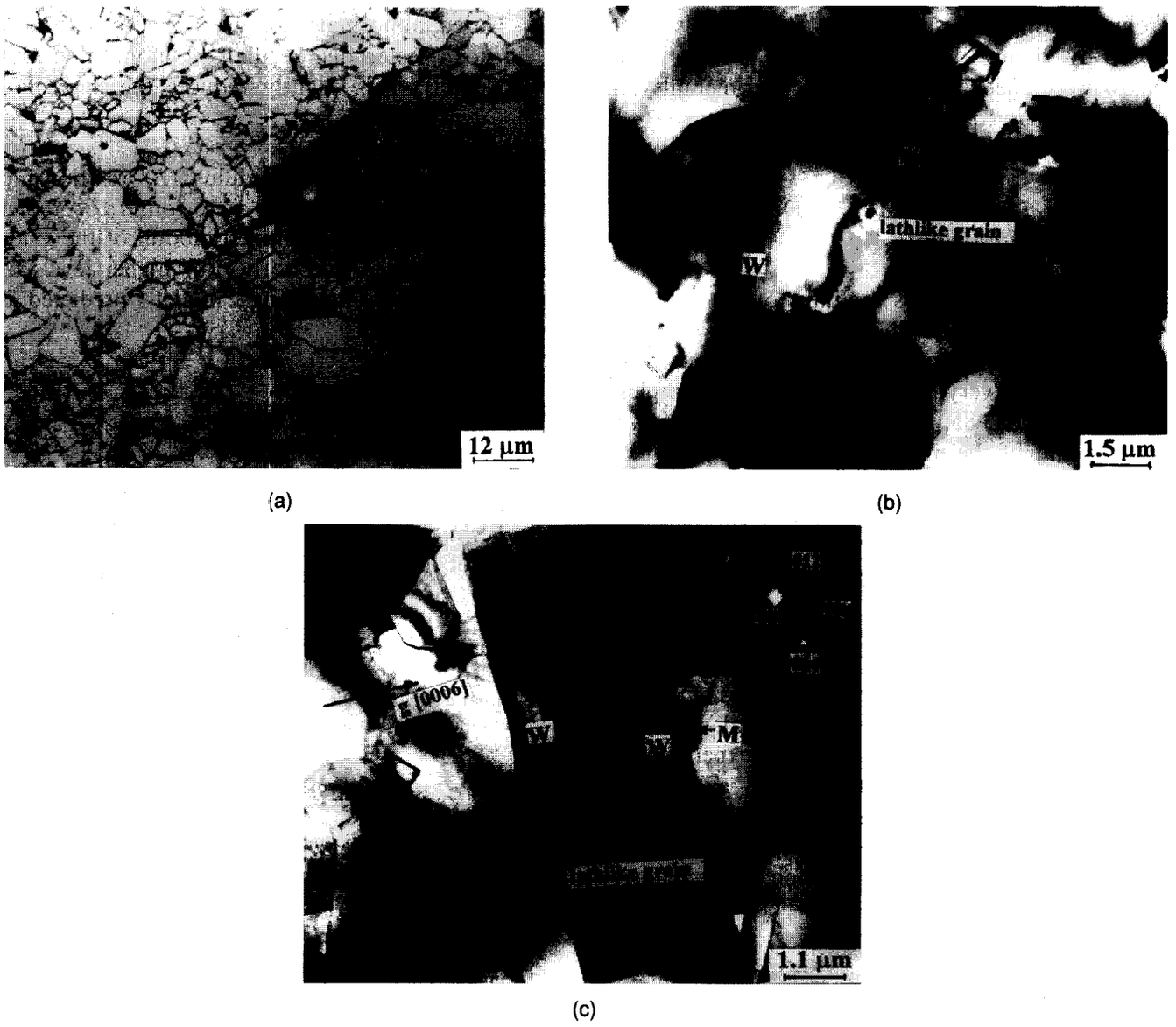

Fig. 8. Microstructure of 400 nm particle size alumina (AES): (a) optical micrograph of thermally etched sample (the Vickers indent is unrelated to this paper); (b), (c) bright-field TEM micrographs showing various aspect ratios of >2 (b) and >3 (c). Note the impurity phases (murkiness) of the basal facets (marker W) in comparison with the cleanness of the areas (marked C) at the ends of the lath-like grain. Inset is the diffraction pattern from zone axis [1 0 $\bar{1}$ 0].

desirable, sintering these materials by the pressureless route could be preferable.

Abnormal grain growth in Al_2O_3 has been attributed[13] to the anisotropic wetting of grains by the MgO-rich intergranular phase. Grain boundaries with high dihedral contact angles of 140 to 180° — typically the long basal facet — favour more wetting relative to those boundaries in contact at the ends of the lath-like grain. The latter show close to normal dihedral angles of 120°, and could be devoid of any wetting. Figures 8(b) and 8(c) show that the contact points on the basal facets of sintered Al_2O_3 are ill-defined (marked W on the micrographs), possibly due to enhanced wetting. These facets are perpendicular to the [0 0 0 6] **g** vector. Selected area diffraction patterns taken from these regions showed diffuse rings, characteristic of the presence of an amorphous phase. The boundaries at the ends of the laths [marked C in Fig. 8(b)] appear much cleaner, and diffraction patterns from these regions showed no diffuse rings.

Adding 5 vol% of nano-sized SiC particles completely suppresses this anisotropic growth provided the optimal sintering temperature is used; compare Fig. 8(a) with Fig. 4(b) (5 vol% SiC–AES alumina sample).

3.6 Elastic properties

The measured values of E, G and v for the composites are shown in Table 3. Note the reduction of E, G and v for the materials sintered in argon (as a result of higher porosity); 1% porosity leads to a reduction of about 2·9% in E.

Several porosity–Young's modulus relationships have been suggested in the literature. These relationships might permit the evaluation of E just

from porosity measurements. The models proposed by Phani,[15] Duckworth[16] and Wang[17] listed below were checked against the experimental values of E observed in this study:

$$E = E_0(1 - ap)^n \quad \text{(Phani[15])} \quad (3)$$

$$E = E_0 e^{-bp} \quad \text{(Duckworth[16])} \quad (4)$$

$$E = E_0 e^{-(bp + cp^2)} \quad \text{(Wang[17])} \quad (5)$$

where E_0 is the Young's modulus of the material with 0% porosity. In Phani's model, $n \approx 2$ and $1 \leq a \leq 3{\cdot}85$, increasing with reduced porosity; considering the very low porosities of our samples, a was taken as 3·85. In Duckworth's model, $b = 7$ independent of the material. In a development of Duckworth's model, Wang showed that b and c vary according to E/E_0 and the volume fraction of pores. For the highest values of E/E_0 (as would be the case here), Wang gave $b = 0{\cdot}946$ and $c = 2{\cdot}54$.

The E_0 values of the composite materials were calculated according to the law of mixtures, using $E_0 = 401$ GPa[17] for alumina and $E_0 = 483$ GPa[18] for SiC. The porosity values, p, were taken to be (1 – fractional density) for each material.

The models are compared with experimental results in Table 4. All of the models give errors large compared with the variations in E with SiC content and porosity. The reliability of the models is worse when the porosity is high; only Wang's approach gives reasonable values here.

4 Conclusions

High density (≥99·6% theoretical) alumina–SiC 'nanocomposites', with up to 15 vol% SiC, have been fabricated by a pressureless sintering route.

To achieve this, attention is needed to a wide range of experimental variables. The key factors include:

(1) Attrition-milling/freeze-drying in an aqueous medium, to give faster and more efficient powder-blending.
(2) Cold-isostatic pressing (CIP) of prior-consolidated green composites; a pressure of 140 MPa is sufficient.
(3) The use of relatively coarse SiC bedding powder, to promote the effusion of gases from the material being sintered.
(4) Nitrogen rather than argon as a sintering gas, and the use of a static atmosphere.
(5) Close matching of the sintering temperature to the particle size of the alumina powder. Abnormal grain growth (which occurs in monolithic Al_2O_3) is normally suppressed by the SiC in the composites. However, if a higher than optimal sintering temperature is used, abnormal grain growth occurs (though to a lesser degree than in monolithic alumina). This slightly reduces the degree of densification.

The porosity–Young's modulus (E) relationship models that were reviewed were found to predict the experimentally determined moduli of the studied composites fairly poorly. For higher levels of porosity (1·8%) only Wang's model[17] predicted E with any accuracy.

Acknowledgements

This work was supported by the EPSRC under Grant No. J77542. We are grateful to the Cookson Technology Centre, Yarnton, Oxford, UK for the use of their experimental facilities.

References

1. Niihara, K., New design concept of structural ceramics: ceramic nanocomposites. In *The Centennial Memorial Issue of the Ceramic Society of Japan*, **99**[10] (1991) 974–982.
2. Zhao, J., Stearns, L. C., Harmer, M. P., Chan, H. M., Miller, G. A. & Cook, R. F., Mechanical behaviour of alumina–SiC 'nanocomposites'. *J. Am. Ceram. Soc.* **76**[2] (1993) 503–510.
3. Borsa, C. E., Jiao, S., Todd, R. I. & Brook, R. J., Processing and properties of Al_2O_3–SiC nanocomposites. *J. Microsc.*, **177** Prt 3 (1995) 305–312.
4. Anya, C. C. & Roberts, S. G., Indentation fracture toughness and surface flaw analysis of sintered alumina/SiC 'nanocomposites'. *J. Eur. Ceram. Soc.*, **16** (1996) 1107–1114.
5. Smith, S. M., Scattergood, R. O., Singh, J. P. & Karasek, K., Effect of silica and processing environment on the toughness of alumina composites. *J. Am. Ceram. Soc.*, **72**[7] (1989) 1252–1255.
6. Coble, R. L., Sintering alumina: effect of atmosphere. *J. Am. Ceram. Soc.*, **45** (1962) 123–127.
7. Uretevizcaya, G., Cavalieri, A. L. & Porto Lopez, J. M., Densification improvement of Al_2O_3–SiC_w composites by impregnation. *Ceram. Int.*, **21** (1995) 97–99.
8. Clinton, D. J., *A Guide to Polishing and Etching of Technical & Engineering Ceramics.* Inst. of Ceramics, Stoke-on-Trent, UK (1987), pp. 17–18.
9. Anya, C. C. & Hendry, A., Pressureless (liquid phase) sintering of X-phase and mullite/X-phase powders. *J. Eur. Ceram. Soc.*, **12** (1993) 297–308.
10. Francois, B. & Kingery, W. D., The sintering of crystalline oxides, II. In *Sintering Key Papers*, eds S. Somiya & Y. Moriyoshi. Elsevier, 1989, pp. 467–485.
11. Vasilos, T. & Rhodes, W., Solids processing of fine grain ceramics. In *Sintering Key Papers*, eds S. Somiya & Y. Moriyoshi. Elsevier, 1989, pp. 741–773.
12. Bennison, S. J., Grain growth. In *Engineering Materials Handbook, Ceramics & Glasses*, **4** (1991) 304–312.
13. Bateman, C. A., Bennison, S. J. & Harmer, M. P., Mechanism for the role of MgO in the sintering of Al_2O_3 containing small amounts of a liquid phase. *J. Am. Ceram. Soc.*, **72**[7] (1989), 1241–1244.
14 O'Donnell, H. L., Readey, M. J. & Kovar, D., Effect of glass additions on the indentation-strength behaviour of alumina. *J. Am. Ceram. Soc.*, **78**[4] (1995) 849–856.

15. Phani, K. K., Young's modulus–porosity relation in gypsum systems. *Am. Ceram. Bull.*, **65**[12] 1584–1586.
16. Duckworth, W., Discussion on compression strength of porous sintered Al_2O_3 and ZrO_2. *J. Am Ceram. Soc.*, **36** (1953) 68.
17. Wang, J. C., Young's modulus of porous materials, Prts I & II. *J. Mater. Sci.*, **19** (1984) 801–814.
18. Lehman, R. L., Overview of ceramics design and process engineering. In *Engineering Materials Handbook. Ceramics & Glasses*, **4** (1991) 29–37.